Sponsored By:
American Institute of Aeronautics and Astronautics (AIAA)
Society of Automotive Engineers (SAE)
American Society of Mechanical Engineers (ASME)

AIAA-80-1290
The Effect of Local Parameters on Gas Turbine Emissions

C. W. Kauffman, S. Correa and N. Orozco, University of Michigan, Ann Arbor, Mich.

AIAA/SAE/ASME 16th JOINT PROPULSION CONFERENCE

June 30-July 2, 1980/Hartford, Connecticut

For permission to copy or republish, contact the American Institute of Aeronautics and Astronautics-1290 Avenue of the Americas, New York, N.Y. 10019

THE EFFECT OF LOCAL PARAMETERS ON GAS TURBINE EMISSIONS*

C.W. Kauffman**, S.M. Correa†, and N.J. Orozco†
The University of Michigan
Ann Arbor, Michigan 48109

Abstract

Gas turbine engine inlet parameters reflect changes in local atmospheric conditions. The pollutant emissions for the engine reflects these changes. In attempting to model the effect of the changing ambient conditions on the emissions it was found that these emissions exhibited an extreme sensitivity to some of the details of the combustion process such as the local fuel-air ratio and the size of the drops in the fuel spray. Fuel-air ratios have been mapped under nonburning conditions using a single JT8D-17 combustion can at simulated idle conditions, and significant variations in the local values have been found. Modelling of the combustor employs a combination of perfectly stirred and plug flow reactors including a finite rate vaporization treatment of the fuel spray. Results show that a small increase in the mean drop size can lead to a large increase in hydrocarbon emissions and decreasing the value of the CO-OH rate constant can lead to large increases in the carbon monoxide emissions. These emissions may also be affected by the spray characteristics with larger drops retarding the combustion process. Hydrocarbon, carbon monoxide, and oxides of nitrogen emissions calculated using the model accurately reflect measured emission variations caused by changing engine inlet conditions.

Nomenclature

c	specific heat of gas
C_D	drag coefficient
g	gravitational acceleration
k	thermal conductivity of gas
L	latent heat of vaporization
$\dot{m}_f$	forced vaporization rate
$\dot{m}_s$	static vaporization rate
Pr	Prandtl number
Q	heat of combustion
Re	Reynolds number
r	fuel-air ratio
t	time
V_a	air velocity
V_f	fuel drop velocity
V_{rel}	relative velocity
Y_O	oxygen concentration
ΔP	pressure drop across can
ΔP_N	pressure drop across nozzle
ΔT	difference between gas temperature and fuel boiling point
ρ_a	density of air
ρ_f	density of liquid

*The work was supported under NASA Grant NSG 3165, NASA Lewis Research Center, Airbreathing Engines Div., David Ercegovic, Contract Monitor.
**Associate Research Scientist, Department of Aerospace Engineering, Member AIAA.
†Graduate student, Dept. Aerospace Engr.

Copyright © American Institute of Aeronautics and Astronautics, Inc., 1980. All rights reserved.

Introduction

The emission levels from a gas turbine combustor are influenced by ambient conditions as well as by internal characteristics which include the spray vaporization, the mixing of the fuel and air and the can aerodynamics. A series of experiments performed by Dils[1] show peak-to-peak gas temperature oscillations from 200°F to 2800°F within the combustor. These results suggest a lack of perfect mixing in the combustor and hence significant variation of the local fuel-air ratios. The experimental part of the work outlined here consists of a study of the mixing process as reflected in the local fuel-air ratio.

The effects of ambient conditions and the spray properties on the emissions were studied with a stirred reactor model. Osgerby[2] has categorized current models of gas turbine combustors as turbulent flame speed models, microvolume burning models or stirred reactor models. Only the stirred reactor models are capable of predicting gross operating characteristics. Sophisticated computer programs are available which model the internal flow-field, the effects of turbulence and jet penetration, and the dynamics of the vaporizing fuel spray coupled with kinetic schemes of differing complexity[3,4]. These models are intended to aid in the design process rather than to predict pollutant levels in the exhaust. Stirred reactor models allow for detailed kinetic schemes without making the numerical calculations intractable. The choice of reactor volumes can be made at various levels of complexity. The stirred reactor model described here was kept straightforward so that the effect of ambient conditions and spray properties could be seen easily. This model combines finite-rate vaporization of the fuel spray with finite rate chemistry to generate consistent temperatures and emissions without requiring large execution times.

Experimental Program

Test Apparatus

The experimental measurements were made in the test rig shown in Fig. 1 which accurately simulates idle conditions for a single JT8D-17 combustor can. The relevant parameters are: $\dot{m}$ = 3.0 lbm/sec, P = 2.5 atm, T = 250°F, and fuel-air ratio = .0117. The air which is supplied by a blow down storage is measured by a choked nozzle and electrically heated. The diffuser section produces a uniform velocity profile, 65 ft/sec, with a turbulence level of approximately 18%. The pressure in the test section is controlled by the addition of air at a choked orifice plate located downstream of the combustor.

As the test rig is cold flow with no combustion occurring the injection and vaporization of Jet A fuel would have been too slow to accurately represent the process in a burning combustor. Instead indoline HO III as supplied by Amoco was substituted. It was heated within a heat exchanger to

250°F at a pressure of 500 psia. As verified by observations with a boroscope the fuel quickly vaporized after injection.

The sampling system consists of a heated four-port probe and a port selector. The four ports are located at radial distances of R = .25, 1.0, 2.0, and 3.0 in. from the center line with the first being designated as R = 0. The probe may be translated in the z direction along the axis of the combustor can and in the θ direction sweeping out each combustor plane. The fuel-air ratio of the sample was measured using a Scott Flame Ionization Detector, FID, or a Lambda Scan Equivalence Ratio Meter. The FID measured unburned hydrocarbons in a sample, and since hydrocarbons and air are the only constituents, the fuel-air ratio is easily calculated. The FID is only capable though of measuring a maximum of 100,000 ppm of hydrocarbons. The Equivalence Ratio Meter was thus acquired so that measurements could be made well into the primary zone, where there is a higher concentration of fuel. Its operation is based on the measurement of residual oxygen concentration after a sample has been mixed with additional air and burned[5].

Testing Methodology

The air and fuel flows were set and the probe was placed at a desired axial combustor location with the exit plane being considered as the point of origin. Measurements were then made for each of the four radii at every 10° around the plane. The relationship between the sampling locations and the combustor geometry is given in Fig. 2.

Experimental Results

Representative fuel-air ratio data is shown in Figs. 3 to 11. In the first three figures the value of the fuel-air ratio is given for the exit, 7 in. and 11 in. planes, for all four radii, and for all angular positions. At the exit plane the fuel-air ratio variation is minimal as of course is demanded by turbine inlet temperature uniformity considerations. However, as one moves upstream variations in the fuel-air ratio becomes more severe even though the 7 in. plane is upstream of a major air inlet location. Generally speaking, as one would expect, the variations are least for small radii. The lack of cylindrical symmetry is perhaps somewhat surprising with variations in the fuel-air ratio of as much as 100% for a 10° azimuthal change. This effect is perhaps most clearly shown in the next two at 5 in. and 9 in. planes, Figs. 6 and 7, where the fuel-air ratio has been averaged over the different radii. If this type of plot is examined for all planes one finds, for example, a consistent fuel deficit in the vicinity of 100° and a fuel surplus in the vicinity of 300°. Interpolation of the data for an entire plane gives results such as in Figs. 8 to 11. The height of the plot (at present unscaled) gives the fuel-air ratio and the azimuthal as well as the polar perspective is indicated. These plots effectively show the fuel-air ratio variation with perhaps a somewhat surprising uniform region near the edge. The data may be quantized to some extent as in Table I. For each plane the average value of the fuel-air ratio has been calculated as well as the standard deviation. If the standard deviation is normalized as in the last column, a meaningful comparison between planes is possible in that a large value of this quantity indicates larger variations in the fuel-air ratio. The three planes with the smallest values are the exit and the planes between dilution ports B and C on Fig. 2. The largest values of the parameter occur for planes located downstream of major dilution ports D and B. The experimental measurements indeed seem to indicate that the fuel-air ratio within a combustor is far from uniform.

TABLE I. AVERAGE AND STANDARD DEVIATION OF THE FUEL-AIR RATIO

Plane	Average Fuel/Air Ratio, f/a	Standard Deviation, σ	$\frac{\sigma}{f/a}$
Exit	.0089	.0012	13.8
5	.0122	.0029	24.0
7	.0182	.0027	14.2
9	.0182	.0023	15.4
11	.0230	.0072	26.6
13	.0457	.0100	21.85

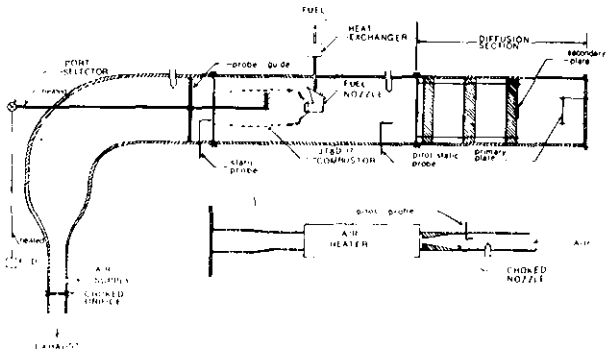

Figure 1. Experimental Apparatus

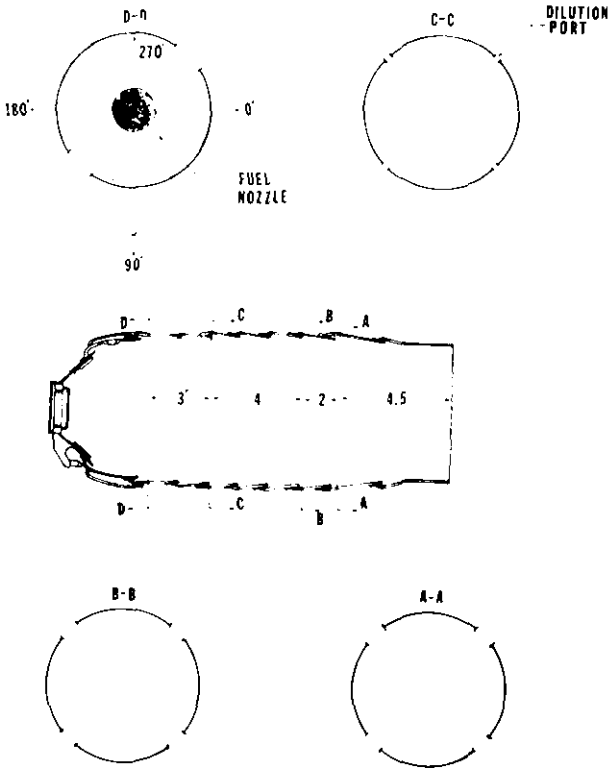

Figure 2. Combustor Geometry

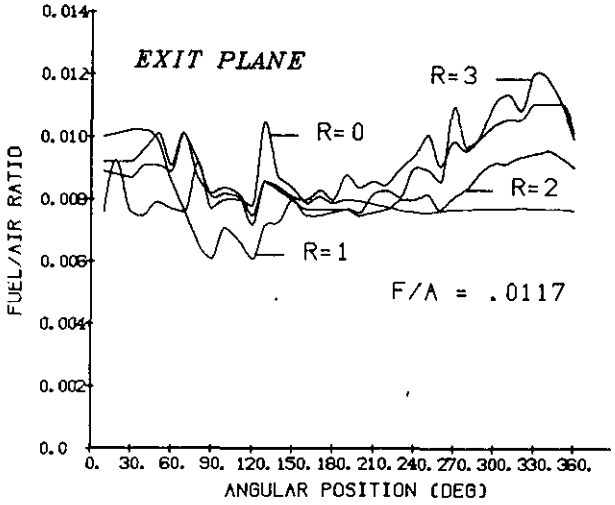

Figure 3. Fuel-Air Ratio at Exit Plane

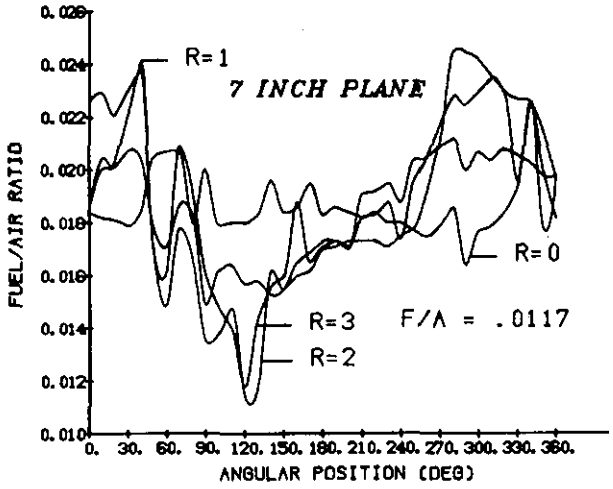

Figure 4. Fuel-Air Ratio at 7" Plane

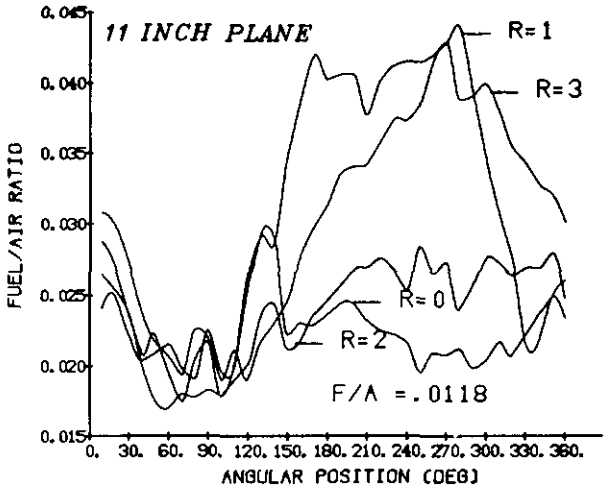

Figure 5. Fuel-Air Ratio at 11" Plane

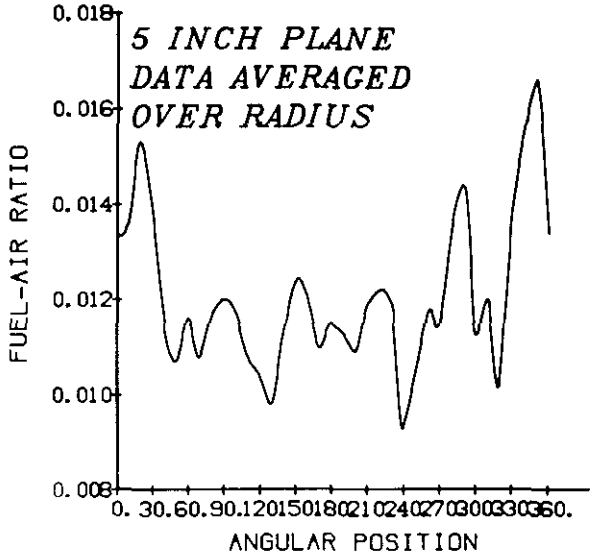

Figure 6. Average Fuel-Air Ratios at 5" Plane

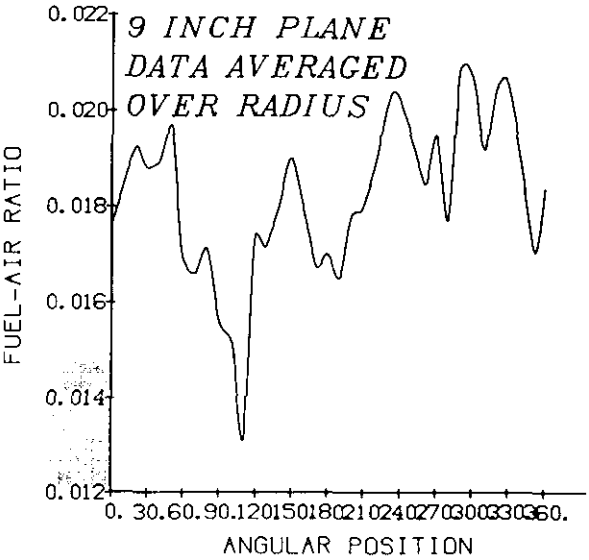

Figure 7. Average Fuel-Air Ratio at 9" Plane

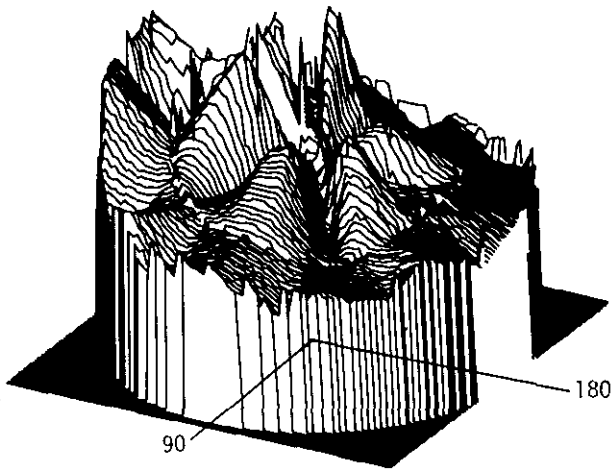

Figure 8. 3-D Fuel-Air Ratio for 5" Plane
Rot. = 210°; Elev. = 25°

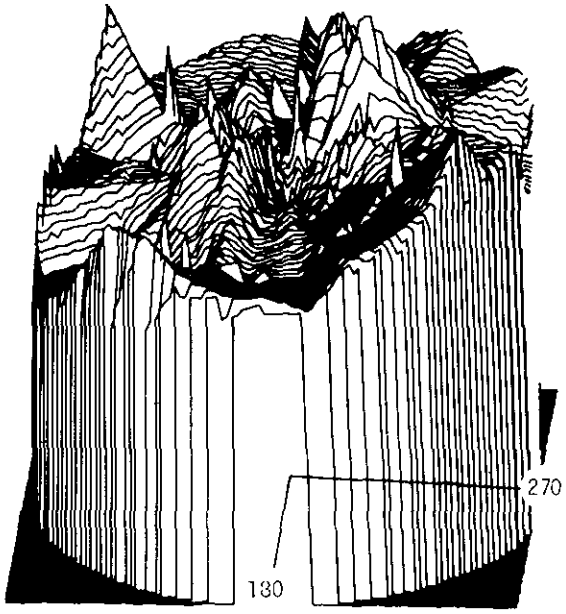

Figure 9. 3-D Fuel-Air Ratio for 9" Plane Rot. = 275°; Elev. = 25°

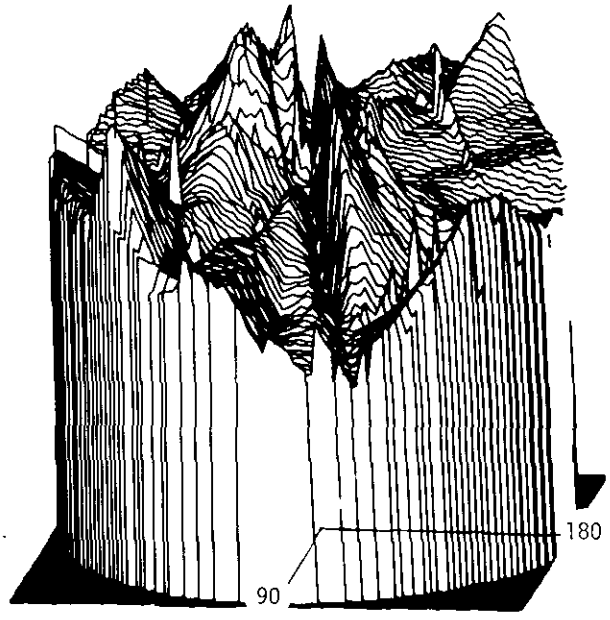

Figure 10. 3-D Fuel-Air Ratio for 11" Plane Rot. = 190°; Elev. = 15°

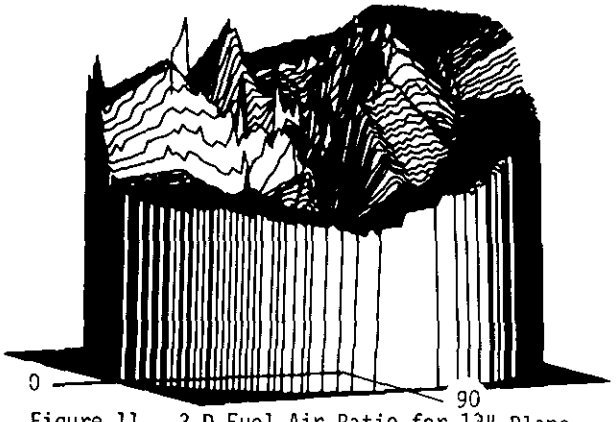

Figure 11. 3-D Fuel-Air Ratio for 13" Plane Rot. = 155°; Elev. = 7°

Analytical Effort

Emission Data

The goal of the analytical portion of this study is to predict emission levels of hydrocarbons (HC), carbon monoxide (CO), and oxides of nitrogen (NOx) as a function of changing ambient conditions for a JT8D-17 operating at idle thrust. Measured emission data previously obtained by Kauffman et al.[6] is given in Table II for a hot, dry day (120°F, 0% relative humidity), for a hot wet day (120°F, 100% relative humidity), and a cold, dry day (-20°F, 0% relative humidity). The results show that the hydrocarbon and carbon monoxide emission index increase more rapidly with ambient humidity increases than with ambient temperature decrease, and that the oxides of nitrogen emission index decreases more rapidly with humidity increase than with temperature decrease. Also, as the fuel-air ratio increases hydrocarbons and carbon monoxide decrease and the oxides of nitrogen increase.

TABLE II. EXPERIMENTAL EMISSION DATA

Pressure Ratio = 2

	f/a = 0.011			f/a = 0.015		
	120°F RH=0	120°F RH=1	-20°F RH=0	120°F RH=0	120°F RH=1	-20°F RH=0
EI-HC	28.0	75.0	46.0	12.0	40.0	25.0
CO	87.0	135.0	115.0	65.0	105.0	95.0
NO	0.9	0.5	0.6	1.1	0.5	0.7
NOx	2.2	0.8	1.4	2.5	0.8	1.5

The combustor inlet air flow is largest on the cold dry day and least on the hot wet day. Because the fuel-air ratio is a constant, the fuel flow rate has the same trend. If the primary fuel nozzle alone is operating, a higher fuel flow rate is the result of a larger pressure drop across the nozzle which leads to improved atomization of the fuel, i.e. a smaller Sauter Mean Diameter (SMD). The SMD is thus expected to be largest on the hot wet day and smallest on the cold dry day. Fuel flow in both the primary and secondary nozzle is more difficult to characterize, so the bulk of the analytical work has been done for a pressure ratio of two, as here only the primary nozzle was in operation.

Vaporization Model

Hydrocarbon emissions may be calculated by considering the vaporization of fuel drops as they pass through a high temperature environment matching that within a combustor. The process of the evaporation of a fuel spray was carefully detailed by Marchionna[7]. The static vaporization rate for a drop of diameter D

$$\dot{m}_s = \frac{2\pi kD}{c} \ell n \left[1 + r\, Y_o \left(1 + \frac{Q}{L}\right) + \frac{c\Delta T}{L}\right]$$

is enhanced by the droplet injection velocity according to

$$\dot{m}_f = \dot{m}_s \left(1 + 0.276\, Re^{0.5}\, Pr^{0.33}\right)$$

where for burning conditions Pr = 0.7. The initial relative velocity between the drop and the air in the combustor is given by

$$V_{rel}^2 = V_a^2 + V_f^2$$

where

$$V_f^2 = c_1 \, g \, \Delta P_N / \rho_f$$

and

$$V_a^2 = c_2 \, g \, \Delta P / \rho_a$$

c_1 and c_2 being empirical constants. The relative velocity of course decreases due to drag forces on the drop and is given by

$$\frac{dV_{rel}}{dt} = \frac{3}{4} \frac{C_D}{D} \frac{\rho_a \, V_{rel}^2}{\rho_f}$$

where

$$C_D = \frac{28}{Re^{0.85}} + 0.48$$

The spray is modelled as a Rosin-Rammler distribution, but the exact distribution could be used if available. The size range is divided into 21 groups each represented by its median diameter. The vaporization rate is computed for each group and is assumed to be constant for 0.1 ms. The pertinent variables in the vaporization equations are then updated. This process is continued for the residence time period in a particular combustor zone or until all the mass in the particular size group has been vaporized. The vaporized part of the spray is considered to be available for the combustion process.

The vaporization model gives realistic hydrocarbon emissions when proper conditions within each combustor zone are specified. For example the effect of residence time on emissions from a primary zone is shown in Fig. 12. As expected a smaller residence time or larger SMD leads to increased emissions. The emission sensitivity to drop size is in good agreement with hydrocarbon emission data obtained by Buchheim[8], Fig. 13 shows the effect of ambient conditions on hydrocarbon emissions. If realistic SMD's are estimated as indicated on the drawing the hydrocarbon emissions follow the trend in Table II.

Bragg Combustor

The Bragg combustor is a gas phase only simulation of a gas turbine combustor using idealized reactors. The primary zone is represented by a perfectly stirred reactor (PSR) and the secondary and dilution zones are represented by plug flow reactors (PFR). In the PSR both axial and lateral mixing are allowed accounting for primary zone recirculation while in the PFR only lateral mixing is allowed. A full kinetic scheme is employed in order to predict the carbon monoxide and oxides of nitrogen emissions. There are of course practically no hydrocarbon emissions. The computational code upon which the model is based, CREK, was originally developed by Pratt and Wormeck[9].

For this model the air flow schedule and reactor volumes are given in Fig. 14. This simulates the JT8D-17 at idle. The fuel is prevaporized and introduced in the primary zone. Initial runs with this model employing reactions 1-17 of the kinetic scheme in Table III gave unrealistically low carbon monoxide emissions. The data in Fig. 15 shows how the predicted carbon monoxide index depends upon the rate constant for reaction 2 ($CO + OH = CO_2 + H$).

TABLE III. KINETIC SCHEME (S.I. UNITS)

FORWARD RATE CONSTANT $k_j = 10^{b_j} T^{n_j} \exp(-T_j/T)$

j							b_j	n_j	T_j
1	C_8H_{16}	O_2	= CO	H_2			8.500	0.0	12200.0
2	CO	OH	= CO_2	H			6.600	0.5	0.0
3	CO_2		M = CO	O	M		12.000	0.0	50353.0
4	H	OH	= H_2	O			6.903	1.0	3525.0
5	H_2O		M = OH	H	M		12.477	0.0	52870.0
6	H	HO_2	= OH	OH			11.398	0.0	957.0
7	OH	H_2	= H	H_2O			10.398	0.0	2618.0
8	H	O	M = OH		M		9.903	0.0	0.0
9	OH	O	= H	O_2			10.398	0.0	0.0
10	H	O_2	M = HO_2		M		9.176	0.0	503.5
11	OH	OH	= H_2O	O			9.778	0.0	503.5
12	OH	N	= H	NO			8.778	0.5	4028.0
13	H	N_2O	= OH	N_2			10.903	0.0	7553.0
14	N	NO	= N_2	O			10.176	0.0	0.0
15	N	O_2	= NO	O			6.778	1.0	3172.0
16	N_2O	O	= NO	NO			11.000	0.0	15000.0
17	N_2O		M = N_2	O	M		11.000	0.0	25176.0
18	NO	HO_2	= NO_2	OH			5.480	1.0	0.0
19	NO_2	H	= NO	OH			11.860	0.0	971.0
20	NO_2	O	= NO	O_2			10.000	0.0	302.0
21	CN	H_2	= HCN	H			10.780	0.0	2667.0
22	HCN	O	= CN	OH			8.150	0.68	8505.0

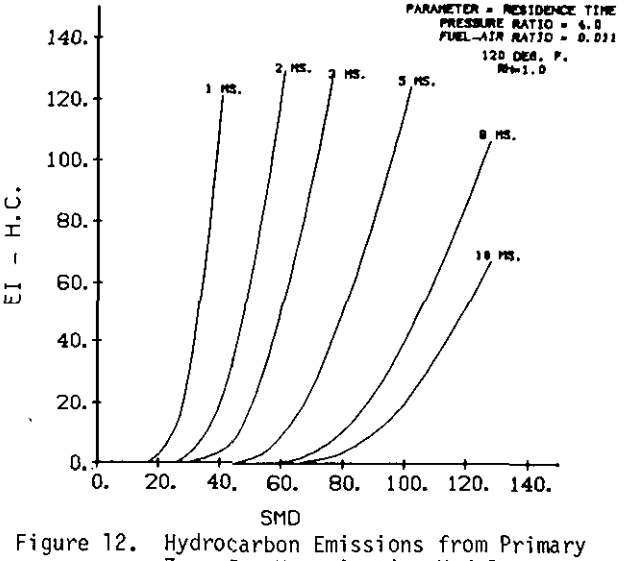

Figure 12. Hydrocarbon Emissions from Primary Zone for Vaporization Model

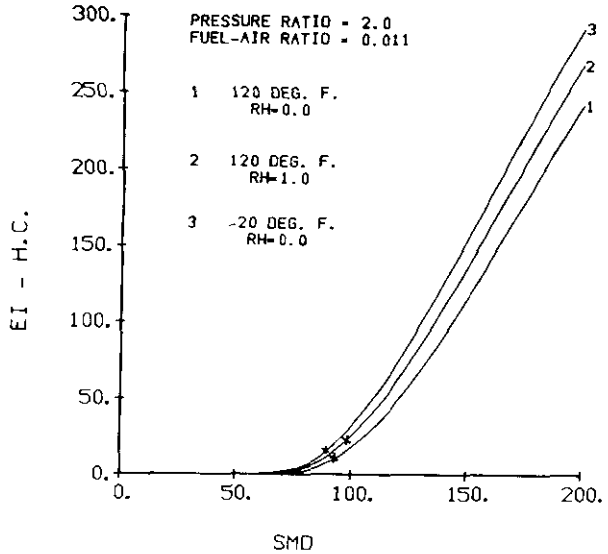

Figure 13. Effect of Ambient Conditions on Vaporization Model

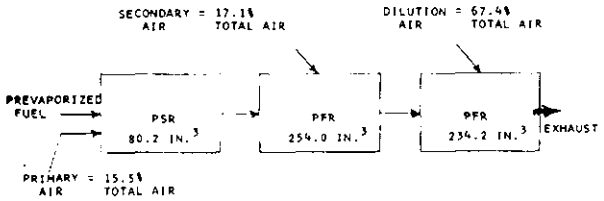

Figure 14. Bragg Combustor Model

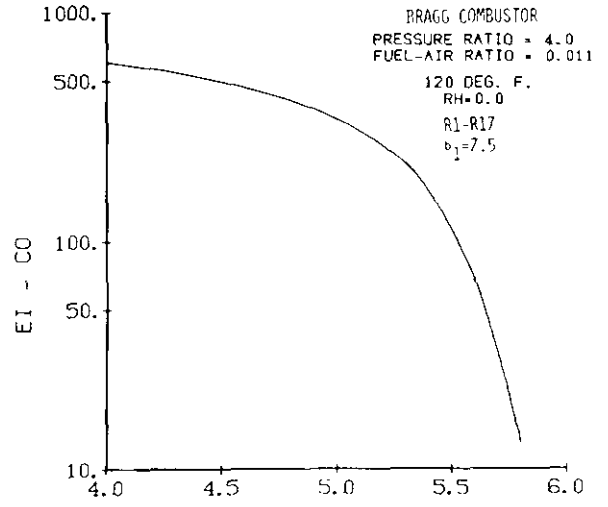

Figure 15. Effect of Rate Constant on Carbon Monoxide Emissions

As the measured emission indices are of the order of 10 to 100 a pre-exponential rate constant of $10^{5.65}$ was employed in further calculations. This rate constant is lower than the values available in the literature. It is also known that carbon monoxide emissions are controlled by the oxidation rate in the secondary and dilution zones rather than by the production rate in the primary zone. As might be expected, an increase in the rate constant for reaction 1 was found to have little effect on increasing the carbon monoxide emissions. As Table IV shows, the Bragg combustor is capable of predicting some results which are of the proper magnitude and trends even at high power conditions.

TABLE IV. BRAGG COMBUSTOR RESULTS

Idle Conditions (PR = 2; f/a = 0.011)
R1-R20, b_1 = 8.50, b_2 = 5.65

Ambient Conditions	120°F RH = 0	120°F RH = 1	-20°F RH = 0
EI-CO	230.3	176.6	293.1
EI-NO	1.209	0.187	0.640
EI-NO_2	0.207	0.033	0.114
EI-NOx	1.416	0.220	0.754

Take-off Conditions (PR = 17.4, f/a = 0.0182)

	Measured	Calculated
EI-CO	0.55	1.38
EI-NOx	24.4	10.4

Coupled Model

In this model vaporization and kinetics have been combined. The amount of vaporization of the fuel drops determines the fuel-air ratio and thus the temperature which then determines the amount of drop vaporization. The iteration scheme for the coupled model, based upon temperature, is shown in Fig. 16. The previously described computational schemes are employed for the vaporization and kinetic calculations. In the limit of small SMD's the Bragg combustor results are reproduced.

For the JT8D-17 the compressor discharge conditions for different engine inlet conditions may be accurately calculated and the air distribution pattern for the combustor has been accurately measured. However, data relating to the fuel spray characteristics is not extensive. Hence, it has been necessary to conduct the calculations treating the SMD as a variable. The SMD's may then be estimated using an appropriate relationship.

Figures 17 to 19 show the emission indices calculated for a fuel-air ratio of 0.015 using reactions R1 through R17 of the kinetic scheme. Using the values of SMD's indicated on the figures

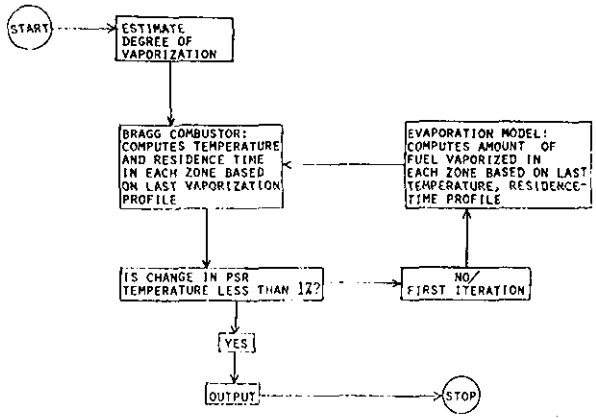

Figure 16. Coupled Combustor Model

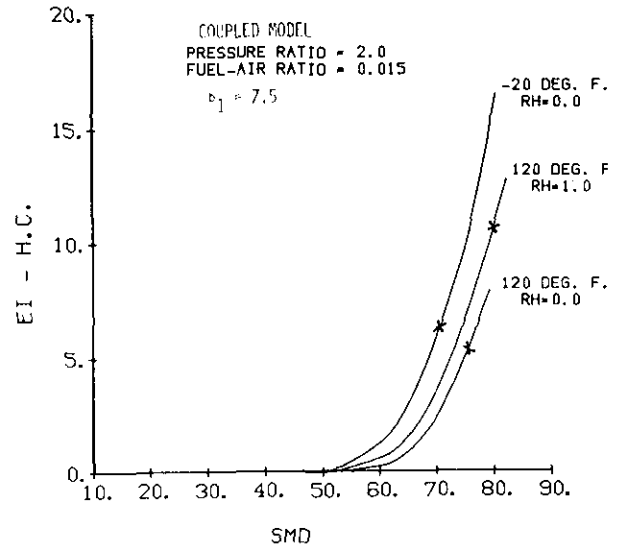

Figure 17. Hydrocarbon Emissions-17 Step Scheme, .015 Fuel-Air Ratio

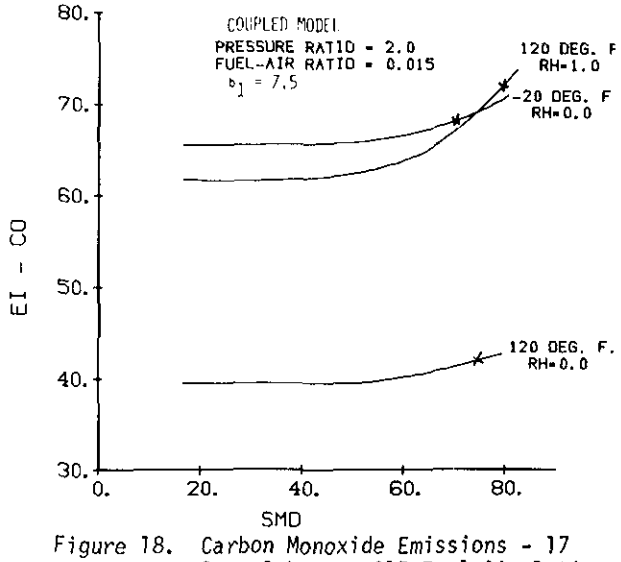

Figure 18. Carbon Monoxide Emissions - 17 Step Scheme, .015 Fuel-Air Ratio

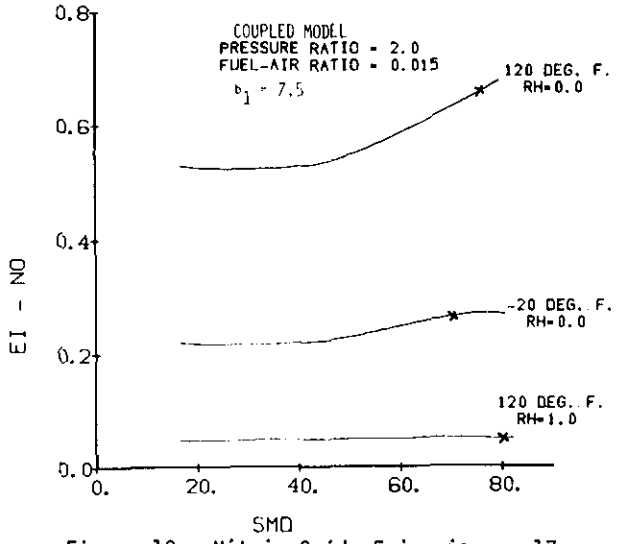

Figure 19. Nitric Oxide Emisssions - 17 Step Scheme, .015 Fuel-Air Ratio

gives the proper ambient trends for the hydrocarbon and carbon monoxide emission indices. The nitric oxide emission index shows the proper trend with ambient conditions regardless of the SMD. For a fuel-air ratio of 0.015 the primary zone is rich. As increasing the SMD decreases the rate of vaporization, the primary zone is driven toward stoichiometric with an attendant increase in temperature clearly leading to an increase in the nitric oxide and ultimately to additional carbon monoxide. Such a trend has been experimentally measured by Buchheim[8] for the regenerated automotive gas turbine

Figures 20 through 22 show the emission indices for an overall fuel-air ratio of 0.011 again using reactions R1 through R17. In this situation the primary zone is near stoichiometric and the effect of retarded vaporization is to make it leaner thus decreasing the flame temperature. The nitric oxides emissions are thereby lowered and the carbon monoxide emissions also decrease. If realistic SMD's are chosen again the hydrocarbon and nitric oxide emission indices show the proper trend while the carbon monoxide emission index on the hot wet day is always too low.

As the experimental data showed that a considerable quantity of nitrogen dioxide was present in the oxides of nitrogen the kinetic scheme was expanded in an attempt account for its production. Figures 23 through 25 show the emission data for a fuel-air ratio of 0.015 using the R1 through R22 kinetic scheme. For these conditions the nitrogen dioxide can be made to account for approximately 20% of the oxides of nitrogen while it was measured to be near 50%. The hydrocarbon and oxides of nitrogen emission indices show the proper trend with ambient conditions (when appropriate SMD's are used) while the carbon monoxide is again too low on the hot wet day.

If the calculations are extended to larger SMD's the coupled model predicts an abrupt increase in the carbon monoxide emission index as seen in Fig. 26. This corresponds to the extinction of the flame in the secondary zone because of the failure of the drops to evaporate. The iterative scheme converges to a nonburning solution. Although the change occurs quite rapidly with SMD the addition of inhomogenities within the combustor would produce a lesser gradient as shown in Buccheim's measurements.

Under leaner conditions of a fuel-air ratio of 0.007 the PSR in the coupled model does not ignite for the cold and wet days unless smaller drops are chosen or the rate constant R1 is increased. The slow rate of vaporization lowers the PSR equivalence ratio below the flammability limit. If the primary zone is modelled as a smaller PSR followed by a PFR the total volumes of which equal the original PSR, as the PSR volume is decreased ignition will occur. However, at present emissions computed under these conditions do not reflect the experimental data.

Liner Model

The carbon monoxide concentration in an actual combustor is observed to peak in the wall region as for example shown by the measurements of Wolters[10]. Its oxidation rate is reduced here because of the lowered local temperature. Through the use of nonhomogenous regions in the combustor it is possible to use a rate constant for reaction R2 which is

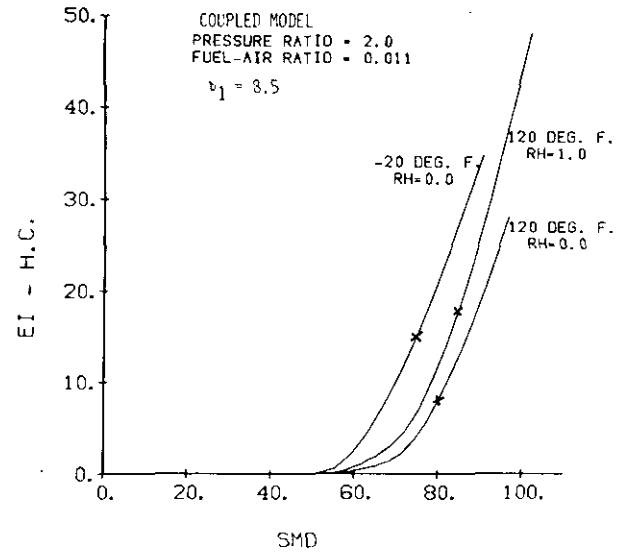

Figure 20. Hydrocarbon Emissions-17 Step Scheme, .011 Fuel-Air Ratio

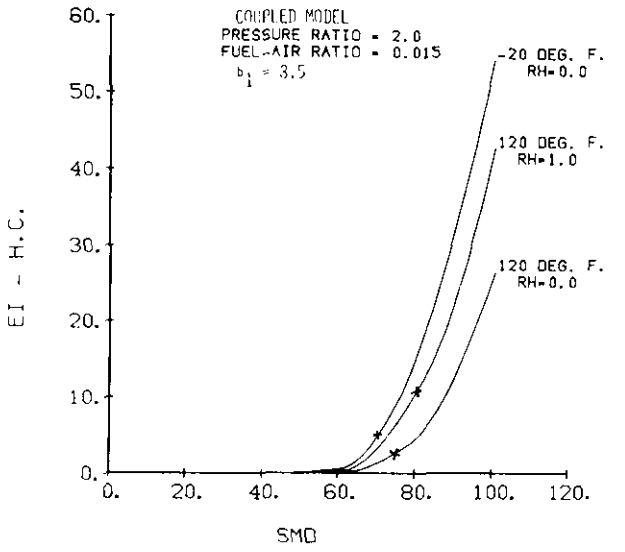

Figure 23. HC Emissions - 22 Step Scheme, .015 Fuel-Air Ratio

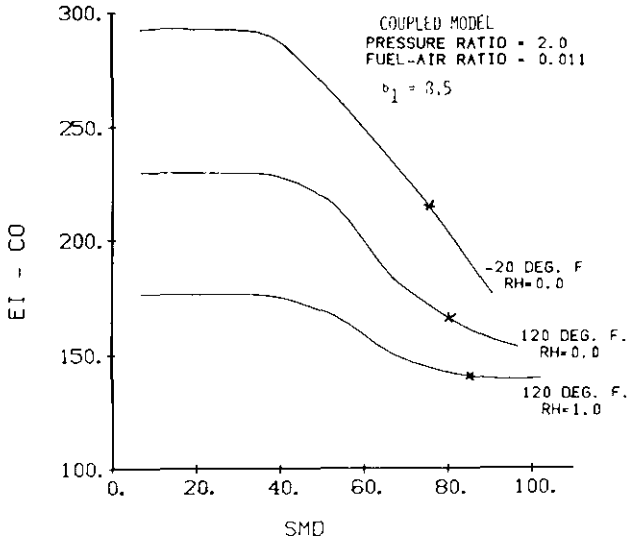

Figure 21. Carbon Monoxide Emissions - 17 Step Scheme, .011 Fuel-Air Ratio

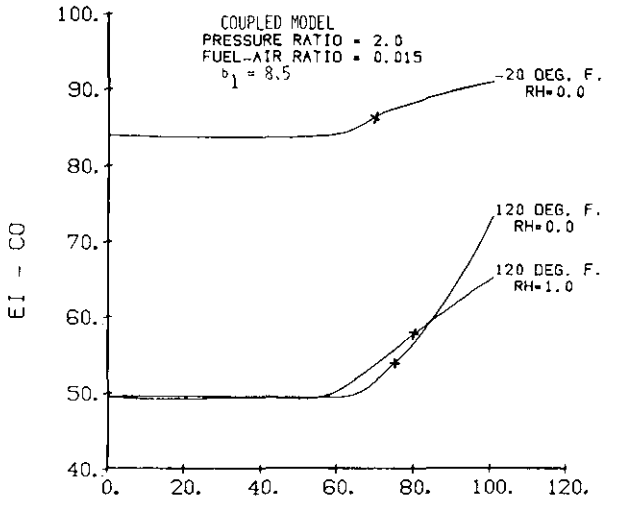

Figure 24. Carbon Monoxide Emissions - 22 Step Scheme, .015 Fuel-Air Ratio

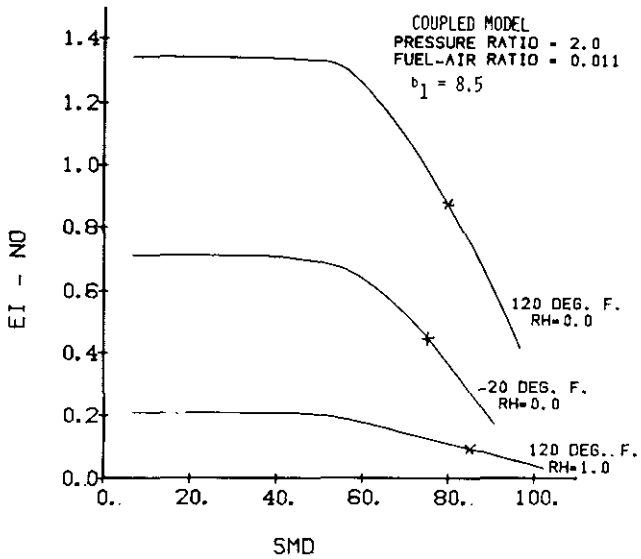

Figure 22. Nitric Oxide Emissions - 17 Step Scheme, .011 Fuel-Air Ratio

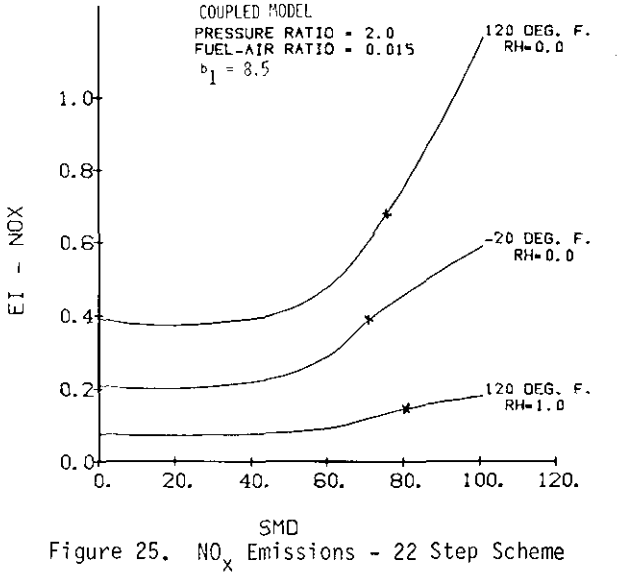

Figure 25. NO_x Emissions - 22 Step Scheme .015 Fuel-Air Ratio

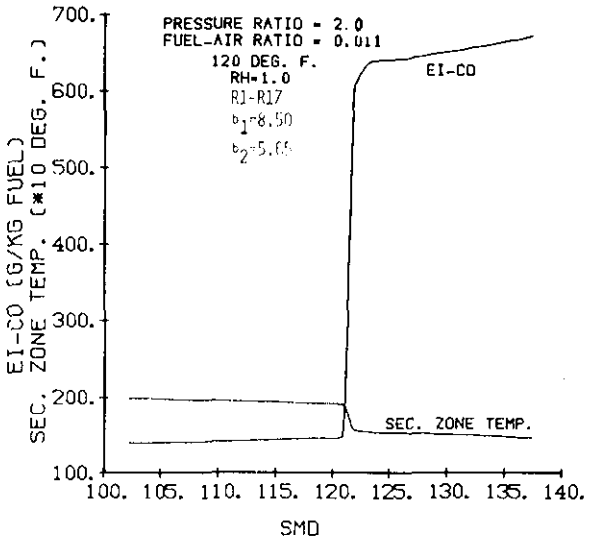

Figure 26. Carbon Monoxide Emissions — Large Fuel Drops

larger and in better agreement with that in the literature. The coupled model has been modified to allow the PSR exhaust to feed into a thin lean liner region and a large richer core region. At present the PSR exhaust diversion, the secondary and dilution air diversion, and the liner and core reactor volumes are input to the model. These quantities are clearly related to can aerodynamics. Reasonable estimates for these quantities do, however, yield realistic levels of carbon monoxide as shown in Table V.

TABLE V. PRELIMINARY RESULTS OF THE NEW MODEL

Condition

PR = 2, f/a = 0.015, cold dry day

R1-R20, b_1 = 8.5, b_2 = 6.6

In the New Model:

Core radius is 93.5% of can radius

5% PSR exhaust feeds into liner

20% of sec., dil. air feeds into liner

	EI-HC	EI-CO	EI-NO	EI-NOx
Coupled Model	7.2	3.91	0.36	0.15
New Model	24.9	29.77	0.43	0.15
Experiment	25.0	95.0	0.70	0.80

Conclusions

Measurements of the local fuel-air ratios within a JT8D-17 combustor can show a high degree of non-uniformity which could affect the emissions significantly. The magnitudes and trends of emissions with varying ambient conditions have been reasonably predicted using a finite vaporization rate stirred reactor model. The model shows that the fuel spray characteristics significantly affect the emissions. Better experimental data is required relating to the spray characterization, combustor can aerodynamics, and the behavior of the primary zone under lean combustion conditions.

Acknowledgments

The authors would like to express their appreciation to N. Marchionna of Avco Lycoming and D.T. Pratt of The University of Michigan for generously making available copies of their computer programs. The efforts of J. Draxler in obtaining the experimental data were also significant.

References

1. Dils, R.R., "Dynamic Gas Temperature Measurements in a Gas Turbine Transition Duct Exit," J. Eng. Power, July 1973.

2. Osgerby, I.T., "Literature Review of Turbine Combustor Modeling and Emissions," AIAA J 12, 6, June 1974.

3. Mosier, S.A. and Roberts, R., "Low-Power Turbopropulsion Combustor Exhaust Emissions," Pratt and Whitney Aircraft Tech. Rept. AFAPL-TR-73-36, July 1973.

4. Bruce, T.W., Mongia, H.C., and Reynolds, R.S., "Combustor Design Criteria Validation," AiResearch Mfg. Co. of Arizona, USARTL-TR-78-55A, March 1979.

5. Haslett, R.A. and Eidson, T.M., "Equivalence Ratio Meter," SAE Paper 770219, SAE Congress and Exposition, Cobo Hall, Detroit, February 28-March 4, 1977.

6. Kauffman, C.W., Subramaniam, A.K., Rogers, D.W., and Claus, R.W., "The Effect of Ambient Conditions on the Emissions of an Idling Gas Turbine," AIAA 16th Aerospace Sciences Meeting, Huntsville, Alabama,Jan. 1978.

7. Marchionna, N., Watkins, S., and Opdyke, G., "Turbine Fuel Tolerance Study," Avco Lycoming, TACOM Rept 12090, October 1975.

8. Buchheim, R., "Untersuchungen zum Emissions verhalten von Pkw-Gasturbinenbrennkammern," Technischen Hochschule Aachen, March 1977.

9. Pratt, D.T. and Wormeck, J.J., "CREK: A Computer Program for Calculation of Combustion Reaction Equilibrium and Kinetics in Laminar or Turbulent Flow," Report WSU-ME-TEL-76-1, Washington State University, March 1976.

10. Wolters, H.R., "Experimenteel onderzoek naar het verbrandingsverloop in een gasturbine verbrandingrkramer en de invloed van water-injectie op de volumuna van stikstofoxiden," Technische Hogeschool, Delft, March 1973.